Progress In Electromagnetics Research, PIER 75, 271–284, 2007

ITERATIVE SOLUTION TO THE NOTCHED WAVEFORM DESIGN IN COGNITIVE ULTRA-WIDEBAND RADIO SYSTEM

L.-L. Zhou and H.-B. Zhu

Lab on Wireless Communication and EMC
Nanjing University of Posts and Telecommunications
Nanjing, China

N.-T. Zhang

School of Electronic and Information Technology
Harbin Institute of Technology
Harbin, China

Abstract—Cognitive Ultra Wideband Radio is proposed to exploit the advantages of combining Cognitive Radio with Ultra Wideband technologies, so as to solve the problems of coexistence and compatibility between UWB and other existing narrowband wireless systems. A novel adaptive UWB pulse shaping algorithm with low complexity, instead of notch filter, is presented for producing the expected spectral notches right in the frequency band occupied by the nearby wireless devices. Simulation results show that the proposed UWB waveform has better single-link BER performances in AWGN channel and stronger anti-jamming ability than other conventional waveforms such as Scholtz's monocycle, etc. Besides, the power spectral density of UWB pulse does not need to be reduced over the whole frequency band. Therefore, it is possible to expand the communication range of UWB systems by increasing the transmitted power of UWB pulse.

1. INTRODUCTION

With the release of the U.S. Federal Communications Commission (FCC) spectral masks in 2002 [1], ultra-wideband (UWB) radios have attracted great interest for their potential applications in short-range high-data-rate wireless communications [2, 3]. With its enormous

band-width, from 3.1 to 10.6 GHz, UWB signaling provides fine temporal resolution and offers the potential for ample multi-path diversity. Baseband UWB systems also enable simple transceiver structures with system-on-chip (SoC) implementations. However, the benefits of UWB signaling may be offset by the interference to and from existing systems (such as GPS, WLAN, and Bluetooth etc.) operating over the same frequency bands.

Narrowband interference (NBI) suppression has been investigated thoroughly for other wide band systems, and mainly for Code Division Multiple Access (CDMA) systems. The suggested solutions include: notch filters before the despreaders [4] or notch antennas in the transmitter [5], and techniques that are incorporated into the despreading operation [6]. Since UWB systems do not sample at Nyquist rate, implementing an analog notch filter requires a bank of analog notch filter digitally is impossible. Moreover, since the NBI center frequency can range from very low frequency to few gigahertz, implementing an analog notch filter requires a bank of analog notch filters, each with different range of possible center frequencies. This approach increases the receiver complexity considerately. So a soft adaptative method of suppressing the NB interference to the UWB devices is needed.

For spectrum overlay control, FCC regulations imposed a spectral mask that strictly constrains the transmission power of a UWB signal to be well below the noise floor over the whole frequency band. On the other hand, the transmission reliability of a UWB system is determined by the received signal-to-noise ratio (SNR), thus requires a technique which makes full use of the allowed power transmission by the FCC mask to maximum the received SNR. Since the spectrum of the transmitted signal is significantly determined by that of the underlying UWB pulse, the choice of the pulse is a key design factor in UWB systems.

The idea of Cognitive Radio (CR) was initially introduced by Joseph Mitolo [7]. CR is defined as a communication system which has the ability to detect other users in the electromagnetic environment and then dynamically alter its power, frequency and other parameters to efficiently utilize vacant spectrum while at the same time avoiding interference to existing systems [8–11]. Therefore, the CR technique could substantial benefit UWB systems by providing collaborative coexistence schemes. On the other hand, UWB technology itself possesses an inherent capability and scalability, suitable for a versatile PHY layer and adaptable to various wireless channel conditions. Taking these factors into account, we aim at exploring a new strategy to exploit the advantages of integrating the cognitive radio with the

UWB technologies to solve the interference problems.

In regard of the ultimate goal of realizing a "perfect" cognitive UWB radio and being capable of configuring itself to any kind of wireless environment and any required transceiver type, we focus on adaptive UWB pulse waveform generation for cooperative spectrum sharing, enabling open access to radio resource with varying degrees of cognitive awareness and intelligent capabilities for increased spectrum utilization. Here, it is targeted to implement a variety of impulsive UWB waveforms and their associated adaptation algorithms, entirely in software-based process and architecture. Such a software-defined UWB radio would be potentially capable of dynamically changing its waveform based upon need, thus reducing the UWB physical layer interface to a software abstraction.

Following this kind of signal waveform adaptation approach in the cognitive UWB (CUWB) radio, a novel design method of pulse waveform optimization based on linear combination of different derivation functions of Gaussian pulse using iterative algorithm is investigated in this paper. The proposed waveform not only achieves a maximum possible transmitted power under FCC mask, but also produces the expected notches right in the frequency band occupied by the nearby wireless devices, so as to significantly suppress the mutual interference. In Section 2, the spectrum sensing of a coexistent system of one UWB and some unknown narrowband devices is presented. According to the spectrum information above, a novel adaptive pulse is suggested in Section 3. The bit error rate (BER) performance using the proposed pulse in UWB system is presented in Section 4. Finally, conclusions are given in the last section.

2. SPECTRUM SENSING OF THE COEXISTENCE SYSTEMS

2.1. TH-BPSK-UWB Signal Model and Its Spectral Analysis

In a single-link UWB communication system, a typical TH-BPSK format of the transmitter output signal is given by [12]

$$S_{tr}(t) = \sum_j d_{[j/N_s]} w(t - jT_f - c_j T_c) \tag{1}$$

where $w(t)$ is the transmitted monocycle. T_f is the pulse repetition time, generally much larger than the monocycle width T_m. $d_{[j/N_s]}$ represents the data modulation, i.e., $\{+1, -1\}$. TH sequence $\{c_j T_c\}$

defines a pseudo-random additional time shift to each monocycle in the pulse train.

Assuming the period of the pulse train $\sum w(t - jT_f - c_jT_c)$ is $T_p = N_pT_f$, the PSD [13] of $S_{tr}(t)$ can be given by:

$$P_{tr}(f) = \frac{\sigma^2}{T_p}|W(f)|^2 + \frac{\mu^2}{T_p^2}\sum_{m=-\infty}^{\infty}\left|W\left(\frac{m}{T_p}\right)\right|^2\delta\left(f - \frac{m}{T_p}\right) \quad (2)$$

Here μ and σ^2 signify the mean and the variance of the sequence $\left\{d_{[j/N_s]}\right\}$ respectively, $W(f)$ is the Fourier transform of Scholtz's monocycle. (2) shows that the PSD of the transmitted signal is composed of a continuous part controlled by the term $|W(f)|^2$, and a discrete part formed by line components at frequency $1/T_p$.

The first-order [14] or second-order [12, 15] Gaussian derivative pulse is often used in the recent research. Scholtz's monocycle, which is similar to the second derivative of the Gaussian pulse, is used here,

$$w(t) = A\left[1 - 4\pi\left(t/\tau\right)^2\right]\exp\left[-2\pi\left(t/\tau\right)^2\right] \quad (3)$$

where A is the amplitude and τ is the pulse shape factor.

2.2. Spectrum Sensing of UWB Received Signal

One of the best schemes to suppress the NBI in UWB system is to produce spectral notches at the central frequency points of the NB systems. Thus, it is necessary to pre-process the signals in the input end of the UWB receiver. Fig. 1 demonstrates the procedure of the

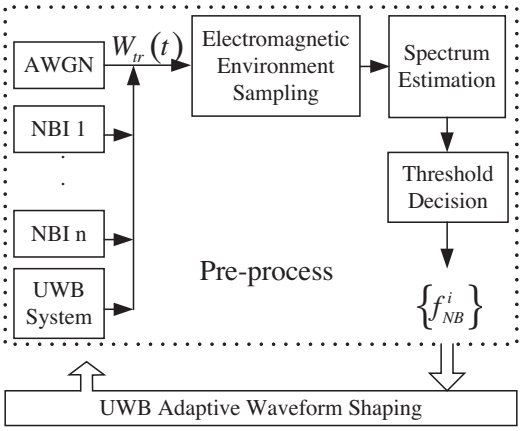

Figure 1. The procedure of UWB adaptive waveform shaping.

pre-process. After sampling the electromagnetic environment in the input of UWB receiver, spectrum estimation and threshold decision are made. Due to the much lower power spectrum and wider band of the UWB system than the NBIs, energy detection [16] is used to obtain the central frequency point of the NBIs.

The input signal of the UWB receiver can be given by

$$W_{tr}(t) = S_{tr}(t) + \sum_i NB_{\{f_{NB}^i\}}(t) + n\,(t)\,, \qquad i = \{1, \ldots N\} \tag{4}$$

where $NB_{\{f_{NB}^i\}}(t)$ represents the ith NB signal with the central frequency $\{f_{NB}^i\}$, and $n(t)$ is additive white Gaussian noise (AWGN).

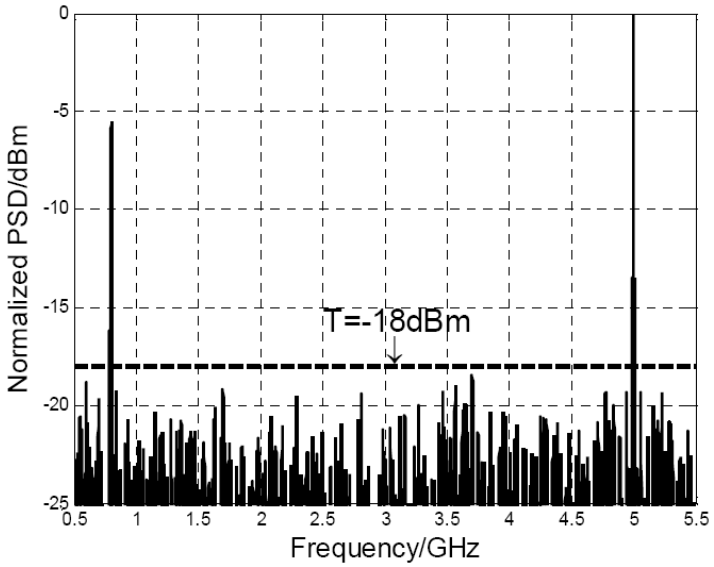

Figure 2. Normalized PSD of the input signals of UWB system.

Figure 2 signifies the normalized PSD of the input signals of UWB system. Given the threshold $T = -18\,\text{dBm}$, it is observed that at least two NBs may cause interference to the UWB system. One of the best methods to suppress the interference is to optimize the base-band pulse waveform to skip the frequency points the NBI systems located.

3. ADAPTIVE PULSE WAVEFORM GENERATION FOR UWB RADIO

Figure 3 gives the normalized PSD for Gaussian derivatives with different parameters. Fig. 3(a) shows that the Gaussian derivatives of higher orders are characterized by higher peak frequency. Differentiation is thus a way to move energy to higher frequency bands. Besides, it can be seen that reducing the value of the pulse shape factor τ shortens the pulse, and thus expands the bandwidth of the transmitted signals.

3.1. Modeling the UWB Adaptive Pulse Signals

Step 1: Setting spectral masks $P_M(f)$. The mask is mainly composed of two parts: 1) FCC restricted the UWB operating bands in the 3.1–10.6 GHz frequency range and regulated UWB power emission in a low level, not more than -41.3 dBm/MHz. 2) The value of PSD corresponding to the frequency $\left\{f_{NB}^{i}\right\}$ of the nearby narrowband system, must be lower than a threshold K so as to suppress the NBI.
Step 2: Modeling the adaptive pulse. A novel pulse shaping optimization based on linear combination of different derivative functions of Gaussian pulse using iterative algorithm to approximate the mask set in Step 1 is investigated in this paper. The proposed waveform has three degrees of freedom: the order of the derivatives n, the shape factor, and the weight vector $\vec{C}$. Different derivatives $\vec{W}$ are set as the Base Functions (BFs), thus the general model of the adaptive pulse can be represented as

$$w(t) = \vec{C}^T\vec{W} = \sum_i c_i w^{(i)}(t),\ \left\{w^{(i)}(t)\,|\tau = \tau_i,\ n = n_i\right\} \tag{5}$$

where $\vec{W} = \left\{w^{(i)}(t)\right\},\ \vec{C} = \{c_i\}$.

3.2. Adaptive Pulse Waveform Shaping

The procedure for selecting the best $\vec{\Gamma}$ and $\vec{C}$ can be described as follows:
Step 1: Initialization. An initial value of $\vec{C}$ is generated in a random way, and is named $\vec{C}_{initial}$. Check if PSD of the linear combination obtained with this coefficient $\vec{C}_{initial}$ meets the limits of spectrum mask $P_M(f)$.
Step 2: Pre-random processing. If the emission limits in Step 1 are met, then skip to Step 3; otherwise, repeat Step 1. It is known that

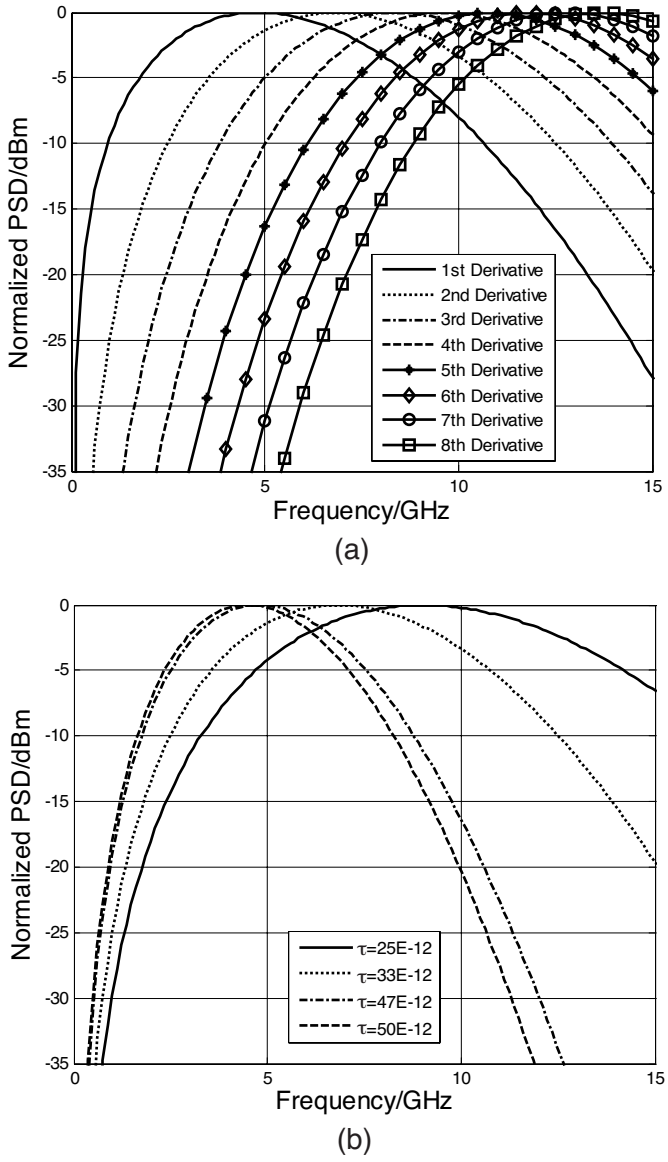

Figure 3. Normalized PSD for Gaussian derivatives with different parameters. (a) Normalized PSD for each order of Gaussian derivative with the same τ. (b) Effect of τ on the normalized PSD for Scholtz's monocycles.

the effect of the parameter $\{\tau_i\}$ of each BF on the combined signal PSD is different. By analysis, it is possible to get a group of satisfied vectors as the shape factors for each BF. The pre-process accelerates the convergence of the iteration in Step 3. Set $\vec{C}_{pre} = \vec{C}_{initial}$.

Step 3: Iteration [17]. The pre-iterative process in Step 2 is not adequate to make an optimal PSD, that is, it has not achieved a maximum possible transmitted power under $P_M(f)$. Using the linearity of Fourier transform, the PSD of combined signal could be pushed much closer to mask. The best weight vector $\vec{C}$ is acquired using iterative algorithm.

First the cutoff condition and the iterative step are set, then the process is initialized by letting $\vec{C} = \vec{C}_{pre}$. Using the iterative step, the coefficient $\vec{C}$ is varied and named as $\vec{C}_{new}$. If $\vec{C}_{new}$ leads to a better waveform than $\vec{C}_{pre}$ and satisfies the cutoff condition, set $\vec{C} = \vec{C}_{new}$. Otherwise, remain $\vec{C} = \vec{C}_{pre}$, and check the cutoff condition. If the iterative result meets the requirement of mask, the iteration is cut off; if not, the step should be changed and then repeat the iteration, till the requirement is satisfied, and name $\vec{C}_{opt} = \vec{C}$.

The cutoff condition of the iteration is given by:

$$\begin{cases} P\Big|_{f=0.5f_{NB}^1} < -41.3\,\text{dBm} \\ P\Big|_{f=f_{NB}^1} < K_1\,\text{dBm} \\ P\Big|_{f=f_{NB}^2} < K_2\,\text{dBm} \\ P\Big|_{f=1.5f_{NB}^{i+1}-0.5f_{NB}^i} < -41.3\,\text{dBm}\ ,\ i = 1,\ldots N \end{cases} \tag{6}$$

where the threshold value (attenuation coefficient) K_1 and K_2 is set as -90, the central frequencies of the NBIs are $f_{NB}^1 = 0.8\,\text{GHz}$, $f_{NB}^2 = 5\,\text{GHz}$, obtained in Section 2. The results achieved in Step 2 and Step 3 are:

$$\begin{aligned} \vec{\Gamma} &= \{700\ 200\ 120\ 120\ 120\ 120\ 200\ 60\ 60\ 60\}(\text{ps}) \\ \vec{C}_{opt} &= \{0.65305\ 0.04312\ -0.00001\ 1.77139\ -4.43852\ 3.62894 \\ &\quad -0.11367\ -0.00001\ 5.12393\ -8.94852\} \end{aligned}$$

Figure 4 shows the time and spectral characteristics of the proposed adaptive pulse waveform. The PSD is nearly zero around $\left\{f_{NB}^i,\, i = 1, 2\right\}$, thus the analytical expression of the proposed new

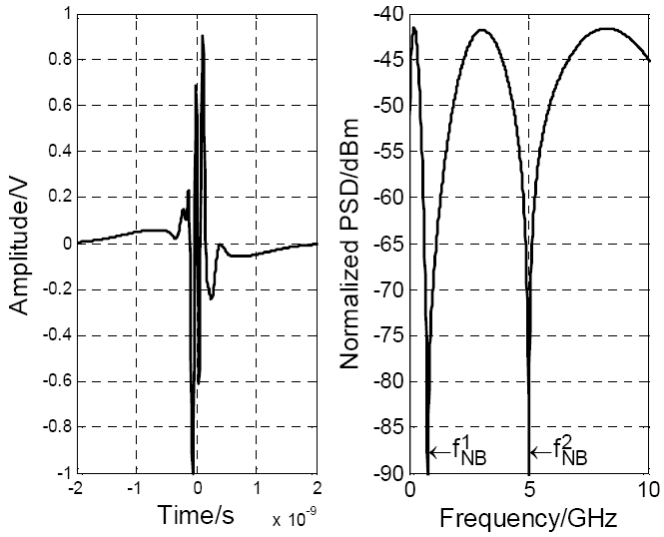

Figure 4. Time and spectral characteristics of the proposed UWB pulse suppressing two NBIs.

waveform is acquired. Given the single NBI in UWB system, the frequency obtained from Section 2 is $f_{NB}^1 = 1.15\,\text{GHz}$, and Fig. 5 shows the time and spectral characteristics of the single adaptive NBI suppression in UWB pulse waveform.

Furthermore, other kind of monocycles can also be chosen as BFs in this algorithm to get the pulse shape upon need.

4. SIMULATIONS AND COMPARISONS

The received signals of the UWB system can be given by

$$S_{rec}(t) = \sum_j A_j d_{[j/N_s]} w_{tr}\left(t - \tau_j - jT_f - c_j T_c\right) + \sum_i x(t)\big|_{\{f_{NB}^i\}} + n(t) \quad (7)$$

where A_j and τ_j signify the path attenuation and time delay respectively. $x(t)\big|_{\{f_{NB}^i\}}$ represents the NBI signals arriving at the receiver end of the UWB system with the central frequency $\{f_{NB}^i\}$ and average power P_{NB}^i. $n(t)$ is AWGN with zero mean and variance $N_0/2$. For convenience, set $A_j = 1$, $\tau_j = 0$ and $N_s = 1$, and use m-sequence as the TH codes. The correlation receiver is chosen in the paper, where the template signal is $v(t) \triangleq w_{tr}(t)$.

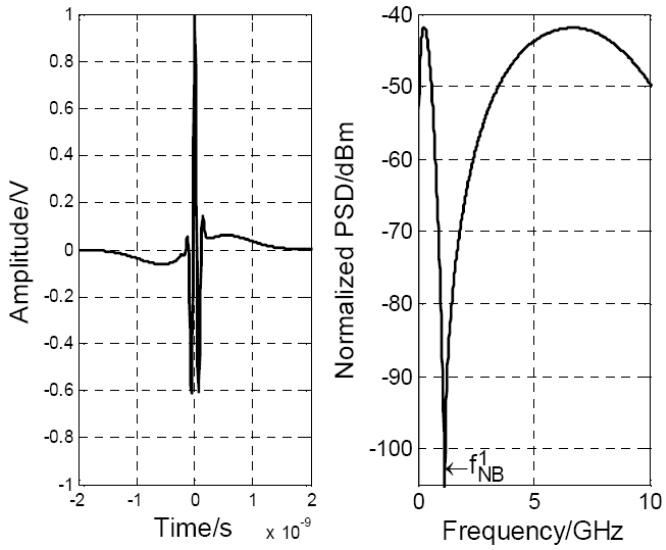

Figure 5. Time and spectral characteristics of the proposed UWB pulse suppressing two NBIs.

The whole interference signals are generally composed of NBIs, the other multiple-access signals and AWGN. Only AWGN and NBIs are considered here. Thus the useful signal is

$$m = \int_{jT_f}^{(j+1)T_f} d_{[j/N_s]} w_{tr}\left(t - iT_f - c_j T_c\right) v\left(t - iT_f - c_j T_c\right) dt \tag{8}$$

and hence the power is

$$m^2 = \int_{-\infty}^{+\infty} w_{tr}^2(t) dt \tag{9}$$

The overall interference signal is given by

$$\begin{aligned} n_{rec}(\mu) &= \int_{jT_f}^{(j+1)T_f} \left[n(t) + \sum_i x(t)\big|_{\{f_{NB}^i\}} \right] v\left(t - iT_f - c_j T_c\right) dt \\ &= \int_{jT_f}^{(j+1)T_f} n(t) v\left(t - iT_f - c_j T_c\right) dt \\ &\quad + \int_{jT_f}^{(j+1)T_f} \sum_i x(t)\big|_{\{f_{NB}^i\}} v\left(t - iT_f - c_j T_c\right) dt \end{aligned} \tag{10}$$

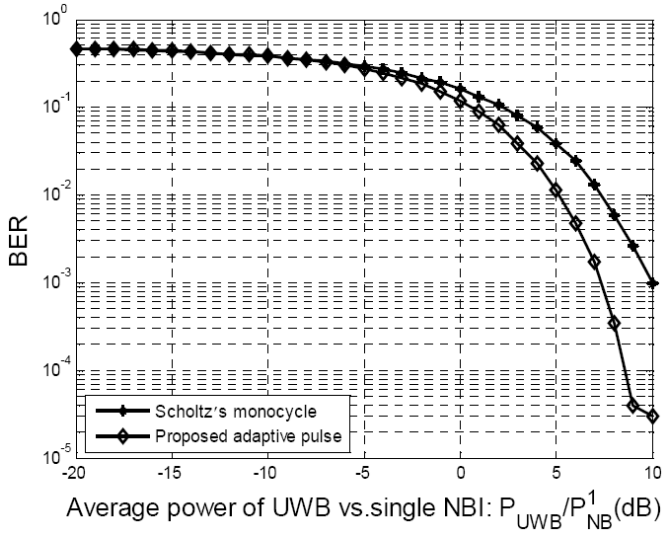

Figure 6. Comparisons of BER performance with single NBI under AWGN channel.

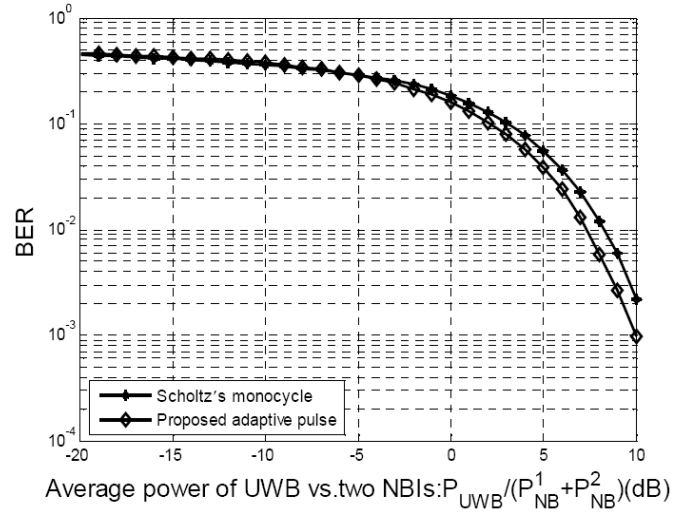

Figure 7. Comparisons of BER performance with two NBIs under AWGN channel.

where $\int_{jT_f}^{(j+1)T_f} n(t)v(t - iT_f - c_jT_c)dt$ is approximate to the Gaussian random variable with zero mean and σ_{rec}^2 variance. Therefore the final signal-to-interference ratio is

$$SIR = m^2 \Big/ \left(\sigma_{rec}^2 + \sum_i P_{NB}^i\right) \tag{11}$$

Comparisons of BER performance with single NBI and two NBIs under AWGN channel are illustrated in Fig. 6 and Fig. 7 respectively. It shows that the proposed adaptive UWB pulse has better single-link BER performance and stronger anti-jamming abilities than other conventional waveforms such as Scholtz's monocycle, etc.

5. CONCLUSIONS

Cognitive Ultra-wideband Radio has been proposed in this paper, so as to exploit the advantages and the unique merits of combining Cognitive Radio philosophy with Ultra Wideband wireless technologies. In regard of the proposed Cognitive UWB Radio, a novel adaptive pulse waveform optimization based on linear combination of different derivative functions of Gaussian pulse are investigated to produce expected notches, instead of notch filters design, in achieving NBIs avoidance as well as matching with the FCC spectral mask. Simulation results show that the proposed adaptive pulse has better BER performances and stronger anti-jamming abilities than other conventional waveforms. It provides good guidance for the future implementations.

ACKNOWLEDGMENT

Supported by NSFC (Key Program) under Grant No. 60432040, NSFC (General Program) under Grant No. 60572024, and Doctoral Fund of Ministry of Education of China under Grant No. 20050293003.

REFERENCES

1. FCC Report and Order, *In the Matter of Revision of Part 15 of the Commission's Rules Regarding Ultra-wideband Transmission Systems*, FCC 02-48, April 2002.
2. Roy, S., J. R. Foerster, V. S. Somayazulu, and D. G. Leeper, "Ultra wideband radio design: the promise of high-speed, short-

range wireless connectivity," *Proc. IEEE*, Vol. 92, No. 2, 295–311, 2004.

3. Chen, C.-H., C.-L.Liu, C.-C. Chiu, and T.-M. Hu, "Ultra-wide band channel calculation by SBR/image techniques for indoor communication," *Journal of Electromagnetic Waves and Applications*, Vol. 20, No. 1, 41–51, 2006.
4. Milstein, L. B., "Interference rejection techniques in spread spectrum communications," *Proc. IEEE*, Vol. 76, No. 6, 657–671, Jun. 1988.
5. Liu, W. C. and C. F. Hsu, "CPW-fed notched monopole antenna for UMTS/IMT-2000/WLAN applications," *Journal of Electromagnetic Waves and Applications*, Vol. 21, No. 6, 841–851, Apr. 2007.
6. Vijayan, R. and H. V. Poor, "Nonlinear techniques for interference suppression in spread-spectrum systems," *IEEE Trans. Commun.*, Vol. 38, No. 7, 1060–1065, Jul. 1990.
7. Mitola, J. and G. Maguire, Jr., "Cognitive Radio: making software radios more personal," *IEEE Personal Communications Magazine*, Vol. 6, No. 6, 13–18 , Aug. 1999.
8. Saeed, R. A., S. Khatun, and B. M. Al, "Ultra-wideband interference mitigation using cross-layer cognitive radio, wireless and optical communications networks," *2006 IFIP International Conference*, 1–5, Apr. 2006.
9. Chakravarthy, V. D., A. K. Shaw, and M. A. Temole, "Cognitive radio — an adaptive waveform with spectral sharing capability," *Wireless Communications and Networking Conference, 2005 IEEE*, Vol. 2, 724–729, 2005.
10. Iacobycci, M. S. and M. G. Di Benedetto, "Radio frequency interference issues in impulse radio multiple access communication systems, ultra wideband systems and technologies," *2002 Digest of Papers, 2002 IEEE Conference*, 293–296, May 2002.
11. Kohno, R., H. Zhang, and H. Nagasaka, "Ultra wideband impulse radio using free-verse pulse waveform shaping, soft-spectrum adaptation, and local sine template receiving," *IEEE*, P802.15-03/097r1, 2003.
12. Win, M. Z., "Ultra-wide bandwidth time-hopping spread-spectrum impulse radio for wireless multiple-access communications," *IEEE Trans. Commun.*, Vol. 48, 679–689, Apr. 2000.
13. Proakis, J. G., *Digital Communications*, 4th edition, Publishing House of Electronics Industry, Beijing, 2001.

14. Zheng, J. Y. and J. M. Lin, "Spectral characteristics of ultra wideband multiple-access signals," *Acta Electronica Sinica*, Vol. 31, No. 10, 1575–1577, 2003.
15. Win, M. Z. and R. A. Scholtz, "Impulse radio: How it work," *IEEE Commun. Lett.*, Vol. 2, No. 2, 36–38, 1998.
16. Chen, J., Y. H. Kuo, and J. D. Li, "Review of automatic communication signals recognition," *Journal of Circuits and Systems*, Vol. 10, No. 5, 102–109, 2005.
17. Zhang, P.-F. and S.-X. Gong, "Improvement on the forward-backward iterative physical optics algorithm applied to computing the RCS of large open-ended cavities," *Journal of Electromagnetic Waves and Applications*, Vol. 21, No. 4, 457–469, 2007.